scientific reports

Check for updates

OPEN

Immune signature and pathways investigation of adrenal gland diffuse large B-cell lymphoma

Weijing Jia[1,4], Ruochen Qi[2,4], Xiaoyan Zhang[2,4], Kepu Liu[2], Longlong Zhang[2], Xiaozheng Fan[2], Bo Yang[3], Guohui Wang[2]✉, Shichao Han[2]✉ & Shuaijun Ma[2]✉

Diffuse large B-cell lymphoma (DLBCL) accounts for approximately 30–40% of all non-Hodgkin lymphoma cases. Organs located DLBCL such as lymph node, stomach, gastrointestinal tract, or skin were reported. However, the adrenal gland DLBCL was not been well explored. We performed RNA sequencing of ten DLBCL samples from adrenal gland, integrated analyzed DLBCL RNA data from multiple organs, defined the new subtypes of adrenal gland DLBCL and explored their molecular signatures. The special expression pattern and microenvironment immunology scores of adrenal glands DLBCL were observed when compared with other organs. Natural killer T cells was predicted to significantly enrichment in adrenal gland DLBCL, canonical cancer pathways such as programmed death protein 1 signaling pathways, tumor necrosis factor signaling pathways and peptide antigen binding pathways were found to be correlated with adrenal gland DLBCL. Further analysis defined two distant adrenal gland DLBCL sub-type by RNA expression pattern. Our study revealed the special expression, defined the molecular subtype of adrenal gland DLBCL. These results expanded the organ related DLBCL data, provided the new knowledge of adrenal gland DLBCL expression profile.

Keywords DLBCL, Adrenal gland, RNAseq, Molecular signatures, Sub-type

Diffuse large B-cell lymphoma (DLBCL) was a common type of non-Hodgkin lymphoma, accounting for approximately 30–40% of all non-Hodgkin lymphoma cases. The incidence of DLBCL varies worldwide, thousands of new cases were diagnosed each year. DLBCL imposed a significant burden on patients and multiple organs symptoms such as swollen lymph nodes, fatigue, night sweats, unexplained weight loss, and fever[1]. Heterozygous symptoms resulted in further complications and finally caused lots of burden and greatly impaired quality of patient's life.

As a heterozygous genetic disease, DLBCL exhibited a wide range of genetic abnormalities including chromosomal rearrangements, gene mutations, and other alterations in signaling pathways regulating cell growth and survival[2]. Over the years, treatment of DLBCL significant progressed including chemotherapy, immunotherapy (such as rituximab), and radiation therapy[3]. Besides, patients were also reported to benefit from stem cell transplantation.

In this study, we report a comprehensive study of DLBCL from adrenal gland and other organs, discovered the specific immune signature and pathways of adrenal gland DLBCL.

Method

RNAseq and bioinformatics

Total RNA was extracted using TRNzol Universal Reagent (4992730, TIANGEN, Beijing, China), and integrity of the RNAs was investigated by Bioanalyzer 2100 system (Agilent Technologies, CA, USA). RNA sequencing was conducted with 1 ug RNA for each sample using the ployA isolation method. More than 5 Giga bases of data per sample was obtained on the Illumina NovaSeq 6000 platform for subsequent analysis.

Clean reads were obtained by removing reads containing adapter and trimming low-quality base using TrimGalore (https://github.com/FelixKrueger/TrimGalore). The reference genome (GRCh38.p13) were downloaded from the Ensembl database (http://ftp.ensembl.org/pub/release-103/fasta/homo_sapiens/dna). The index of the reference genome was built, and paired-end clean reads were aligned to the reference genome by

[1]Department of Hematology, The First Affiliated Hospital of Air Force Military Medical University, Xi'an 710032, Shaanxi, China. [2]Department of Urology, The First Affiliated Hospital of Air Force Military Medical University, No.127, Changle West Road, Xi'an 710032, Shaanxi, China. [3]Department of Urology, The Zheng He Hospital, Xi'an, Shaanxi, China. [4]Weijing Jia, Ruochen Qi and Xiaoyan Zhang contributed equally to this work. ✉email: wghdoctor@126.com; hanshichaohome@163.com; MSJ13488261445@163.com

STAR (v.2.7.10a)[4]. Raw counts were calculated using featureCounts (v2.0.1)[5]. Differential expression analysis was performed using DESeq2 (v.1.16.1)[6]. Genes with an adjusted p value of <0.05 and $|\log2FoldChange| > 1$ were considered as significantly changed in expression.

Public RNA dataset

Counts, Transcript per million (TPM) reads, and clinical features data of Diffuse large B-cell lymphoma (DLBCL) from TCGA (The Cancer Genome Atlas) database were downloaded from the UCSC Xena Data center (https://xenabrowser.net/datapages/?cohort=GDC%20TCGA%20Large%20B-cell%20Lymphoma%20(DLBC)&removeHub=https%3A%2F%2Fxena.treehouse.gi.ucsc.edu%3A443).

Immune microenvironment analysis

The xCell package (v.1.1.0, R language)[7] was used to calculated the scores for immune cell infiltration in DLBCL expression profile of our data and TCGA. The microenvironmental score, immune score and cell sub type (CD4+ T cells, CD8+ T cells, B cells, neutrophils, macrophages, etc.) score were calculated.

Gene set enrichment analysis

The differential expression profile was ordered by log2FoldChange from high to low, then the gene set enrichment analysis (GSEA) was performed by clusterProfiler (v.3.14.3)[8]. Hallmark gene sets (H), GO gene sets (C5), and oncogenic gene sets (C6) were selected for the reference molecular signature database (MSigDB, https://www.gsea-msigdb.org/gsea/msigdb/) to perform gene set enrichment analysis.

Statistical analysis

Normally distributed data were compared by unpaired Student's t-test for two groups comparisons and one-way analysis of variance (ANOVA) for multiple groups. Non-normally distributed data were compared by Wilcoxon-test for two groups comparisons and Kruskal–Wallis test for multiple groups. p values <0.05 were considered significant difference. Data statistically analysis were using GraphPad Prism 5.0 (GraphPad Software., San Diego, CA, United States) and ggpubr (v.0.6.0, R language, https://rpkgs.datanovia.com/ggpubr/).

Result

RNA data of 58 DLBCL [including 48 samples from TCGA and 10 samples from our center (clinical features summarized in Table 1)] were analysis. According to the organs, all samples were further divided into 16 locations, including stomach, lymph nodes, jejunum, breast, small intestine, anterior mediastinum, colon, submandibular gland, thyroid gland, soft tissue, peritoneum, testis, brain stem, bone joints, cerebellum, and adrenal gland. The correlation among all DLBCL cases were calculated, two expression patterns were obtained (Fig. 1A). To investigate the expression pattern related immune microenvironment, all samples immune score was calculated. The overall immune score (Fig. 1B) and microenvironment score (Fig. 1C) showed heterozygous pattern among locations which indicated the organ specific immune microenvironment.

To further investigate subtype of all locations, immune score for each cellular type was calculated and clustered. Specifically, NKT subtype was significantly enriched in adrenal gland samples (Fig. 2A). Further NKT score among locations also demonstrated significant high score for adrenal gland than other locations (Fig. 2B).

According 60.4% (29/48) in all reported DLBCL in TCGA database, lymph nodes was the most common location in DLBCL. To investigated the potential pathway between adrenal gland and lymph nodes, 10 adrenal gland and 29 lymph nodes samples were enrolled for differential gene analysis. 24,782 differential expressed genes were obtained (Fig. 3A,B). Gene set enrichment analysis revealed canonical cancer pathways were found negatively correlated with adrenal gland samples, such as PD1 signaling pathways, TNF signaling pathways and peptide antigen binding pathways (Fig. 3C).

To further specify the molecular subtype of adrenal gland related DLBCL, we re-clustered the adrenal gland into two clusters based on the expression patters (Fig. 4A). Totally, 484 genes differential expressed between cluster 1 and cluster 2, including 383 genes significant high expressed in cluster 1 and 101 genes significant high expressed in cluster 2. Interestingly, majority of the top10 enriched genes in cluster 1 were non-coding RNAs including: LINC02788, REG1A, TPRG1-AS1, FMO6P, LINC02452, LINC02641, LINC01558, FERP1, LZTS1-

Patient	Pathological molecular classification	Pathologic
Patient1	BCL2+, CD20+, CD21+, cMyc > 30%, Ki67 > 90%, MUM1+, PAX5+	Non-GCB DLBCL
Patient2	BCL2+, CD20+, Ki67 > 80%, MUM1+, PAX5+	Non-GCB DLBCL
Patient3	BCL2+, BCL6+, CD20+, CD79a+, CD3+, Ki67 > 75%, MUM1+, PAX5+	Non-GCB DLBCL
Patient4	BCL2+, BCL6+, CD20+, VIM+, Ki67 > 80%, MUM1+	Non-GCB DLBCL
Patient5	CD2+, CD20+, CD79a+, Ki67 > 85%	Non-GCB DLBCL
Patient6	BCL6+, CD20+, LCA+, Ki67 > 90%, MUM1+, VIM+	Non-GCB DLBCL
Patient7	BCL2+, CD20+, PAX5+, CD79a+, LCA+, Ki67 > 90%, MUM1+	Non-GCB DLBCL
Patient8	BCL2+, BCL6+, CD20+, LCA+, CD3+, CD5+, CD7+, Ki67 > 67%, MUM1+	Non-GCB DLBCL
Patient9	BCL2+, BCL6+, CD20+, CD3+, CD30+, Ki67 > 90%, MUM1+, TP53+	Non-GCB DLBCL
Patient10	BCL2+, CD20+, Ki67 > 80%, MUM1+	Non-GCB DLBCL

Table 1. Pathological classification for DLBCL patients.

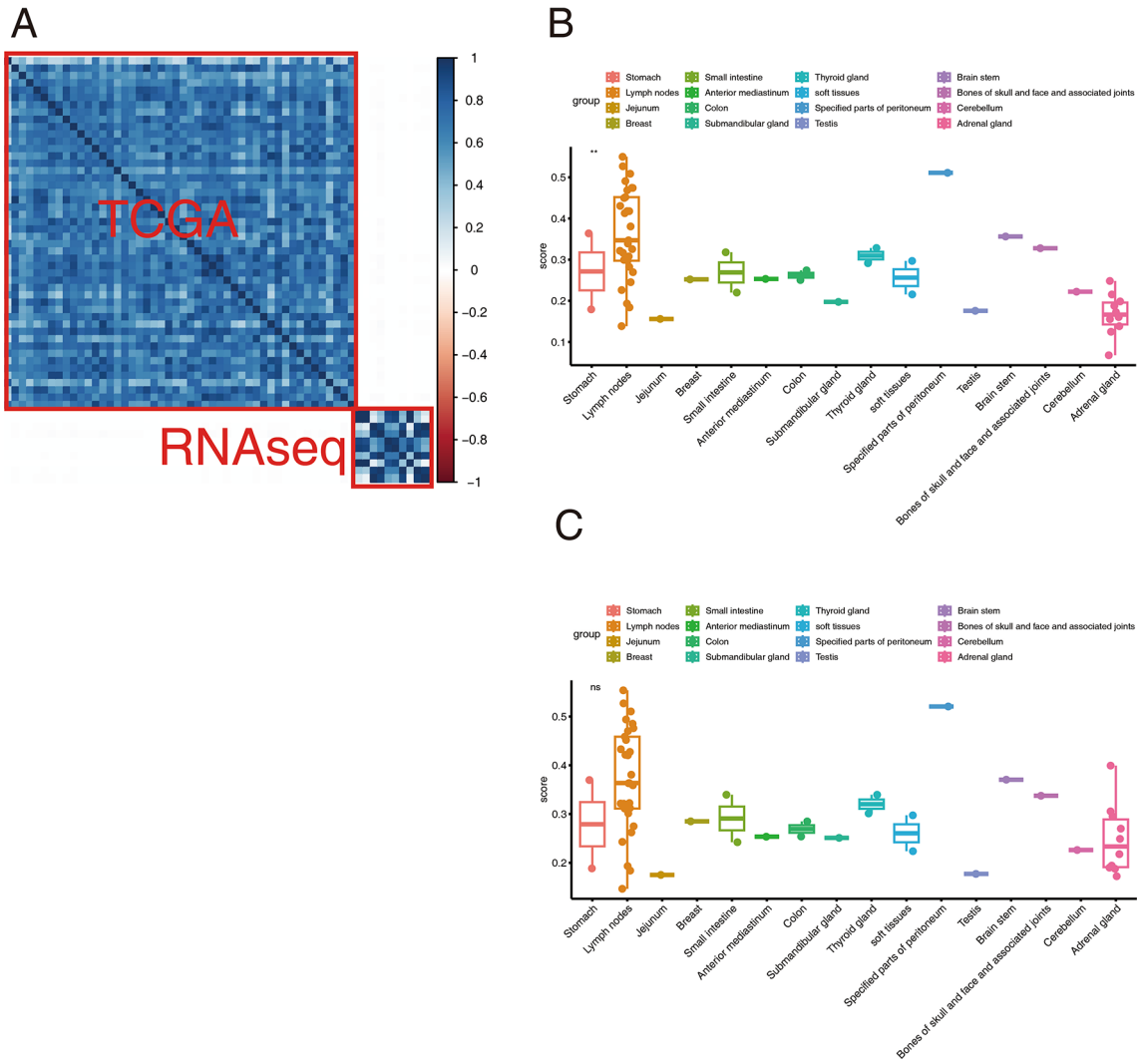

Fig. 1. Expression and immune pattern among organs. (**A**) Correlation plot of all DLBCL samples. Two clusters were observed between adrenal gland from our center and other organs from TCGA database. (**B**) Immune scores of all DLBCL samples. Heterozygous immune scores pattern among among multiple organs. Nonparametric Kruskal–Wallis test was utilized for comparison among multiple groups. p values < 0.05 were considered significant difference. (**C**) Microenviroment score of all DLBCL samples. Heterozygous immune scores pattern among among multiple organs. Nonparametric Kruskal–Wallis test was utilized for comparison among multiple groups. p values < 0.05 were considered significant difference.

AS1 and MAGI1-AS1. The majority of the top10 enriched genes in cluster 2 were protein-coding genes including: CT45A3, PRR23D1, ALPP, ALPG, MIR663B, OPN1MW2, SLC28A2, PRR23D2, NEU2 and KRT2 (Fig. 4B). The NKT score showed no significance between these two clusters (Fig. 4C), however, the CD4 memory score (Fig. 4D) and proliferate B cell score (Fig. 4E) showed higher in cluster 1 and cluster 2 respectively. GSEA analysis indicated KRAS pathways and other classical carcinoma pathways enriched in cluster 2 (Fig. 4F,G).

Discussion

DLBCL encompassed different subtypes and molecular variants that exhibited heterozygous characteristics and clinical behaviors. Main subtype of DLBCL included activated B-cell-like (ABC) DLBCL, germinal center B-cell-like (GCB) DLBCL, primary mediastinal large B-cell lymphoma (PMBCL), and other un-specificities type. Along with the progress of DLBLC, multiple dysfunctions in the immune system could be observed, such as impaired immune surveillance, chronic inflammation, and cell interactions in the tumor microenvironment.

DLBCL typically presented with enlarged lymph nodes, often in the neck, armpit, groin regions, gastrointestinal tract, central nervous system, or other organs. Patients may experience symptoms such as fatigue, night sweats, unexplained weight loss, fever, and generalized symptoms of lymphoma. Risk factors of DLBCL were reported such as age (older individuals), immunodeficiency (such as HIV/AIDS or post-transplant immunosuppression), autoimmune diseases, Epstein-Barr virus, and prior history of other lymphomas.

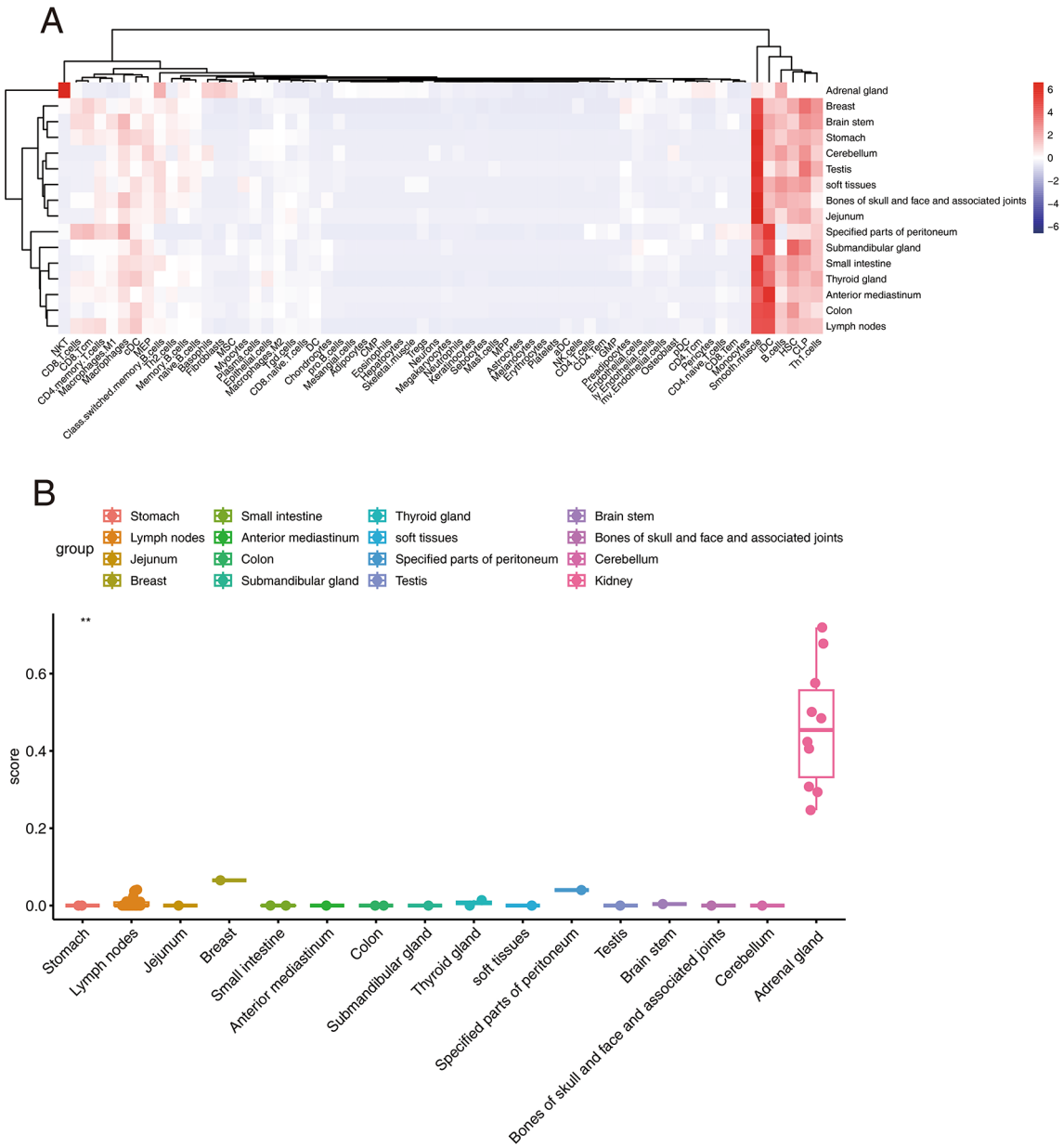

Fig. 2. Expression and immune pattern among organs. (**A**) Heatmap plot of all DLBCL samples. NKT cell score was enriched in adrenal gland samples. (**B**) NKT score of all DLBCL samples. Heterozygous NKT scores pattern among among multiple organs. Nonparametric Kruskal–Wallis test was utilized for comparison among multiple groups. p values < 0.05 were considered significant difference.

The standard treatment for DLBCL was R-CHOP, which involved a combination of chemotherapy drugs and immunotherapy, included rituximab (an anti-CD20 antibody), cyclophosphamide, doxorubicin, vincristine, and prednisone. This approach exhibited high response rates and improved survival outcomes. Besides CD20, CD30-targeted antibody-drug conjugate called brentuximab vedotin also shown promising results in patients with relapsed or refractory DLBCL. Other targeted therapies, such as lenalidomide and ibrutinib, were being investigated in clinical trials. Chimeric antigen receptor (CAR) T cell therapy, which modified the patient's T cells to express a CAR that recognizes and targets CD19, demonstrated complete remissions in relapsed or failed to respond to other treatments patients.

NKT cell, express characteristics of both T cells and natural killer cells, mediated tumor immune-surveillance. Li et al. first performed in vitro studies to investigate NKT cell responses to human B cell lymphoma lines, and found that the addition of α-GalCer to NKT cell/lymphoma co-cultures resulted in the induction of cytokine production by NKT cells[9]. In treated mice, type I iNKT cells produce IFN-γ and played an immunoregulatory role on the NK and CD8+ T cell populations by inducing cytokine production.

The complex network known as the tumor microenvironment (TME) consists of various cellular and noncellular components that create a physical barrier surrounding tumor cells[10]. Recent studies have increasingly

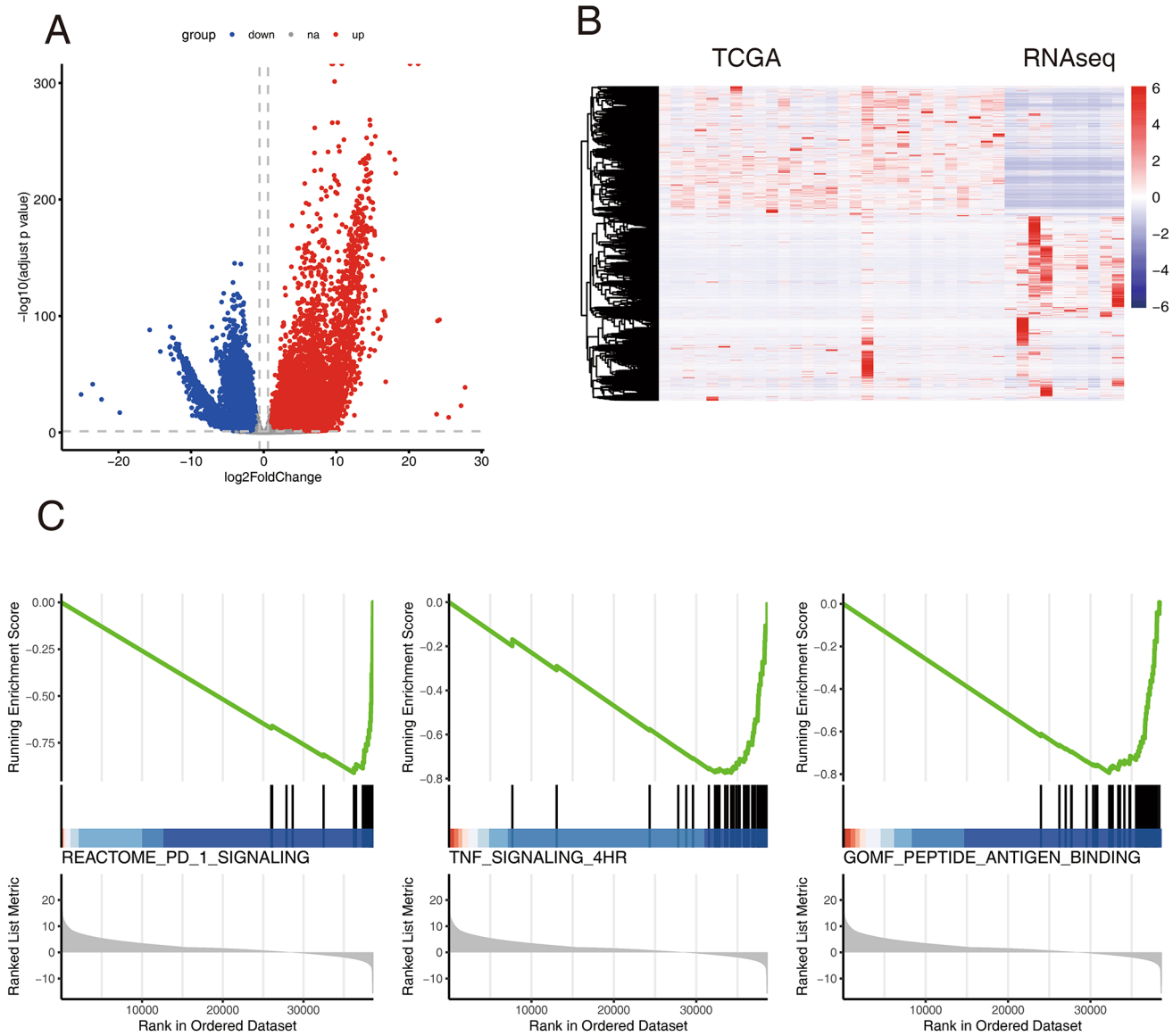

Fig. 3. Differentially expressed genes between adrenal gland and lymph node. (**A**) Dysregulated genes between adrenal gland and lymph node samples, adjusted p value < 0.05, fold change > 1 were selected as thresholds. (**B**) Heatmap of all DLBCL samples including adrenal gland and lymph node. (**C**) Differentially expressed gene enriched in pathways by gene set enrichment analysis.

highlighted the active roles of TME components in the initiation and maintenance of carcinogenesis, challenging the notion that they are mere bystanders[11]. The TME plays a crucial role in multiple biological processes, including pathogenesis, progression, metastasis, and drug resistance, by facilitating sustained proliferation and immune evasion[12]. Given the limited effectiveness of standard therapies in certain patients, researchers have explored TME-based treatments as novel strategies to establish a more immunogenic environment and enhance drug delivery, ultimately improving patient response rates. Emerging evidence suggests that the composition of the TME is pivotal in understanding the pathogenesis of lymphoma, while also providing novel avenues for targeted therapies and tumor prognosis prediction.

The tumor microenvironment (TME) can be classified into two distinct components: the immune microenvironment, primarily composed of immune cells, and the nonimmune microenvironment, which is predominantly governed by fibroblasts[13]. Within the immune microenvironment, various cells such as T and B lymphocytes, tumor-associated macrophages (TAMs), myeloid-derived suppressor cells (MDSCs), tumor-associated neutrophils (TANs), natural killer (NK) cells, dendritic cells (DCs), and others, contribute to the establishment of an immunosuppressive microenvironment and aid in evading immune responses. On the other hand, the nonimmune microenvironment primarily consists of stromal cells, including cancer-associated fibroblasts (CAFs), extracellular matrix (ECM), pericytes, mesenchymal stromal cells, and other secreted molecules such as growth factors, cytokines, chemokines, and extracellular vesicles[14]. These TME cells exhibit distinct biomarkers and fulfill various roles in the tumorigenesis and prognosis of B-cell lymphoma.

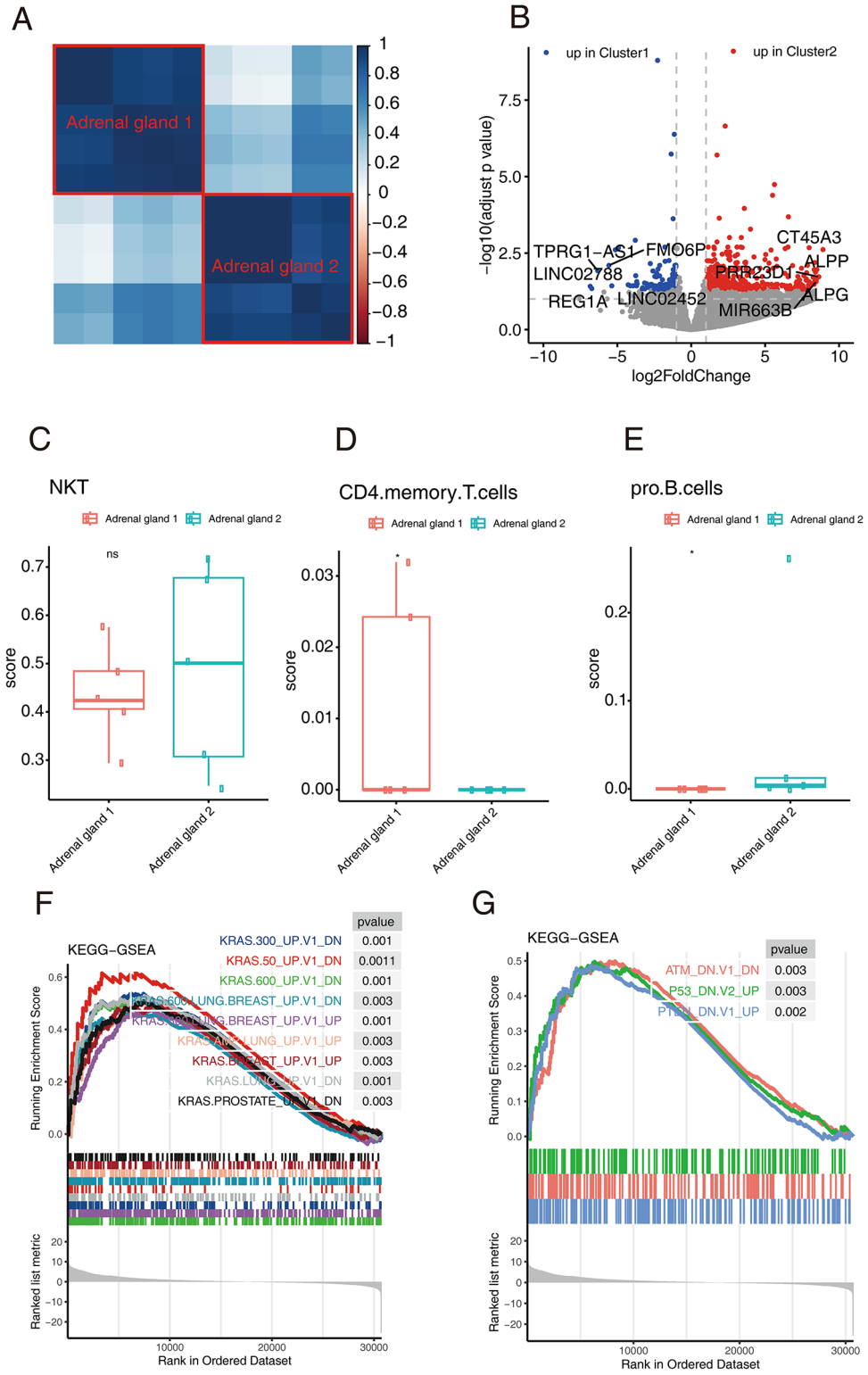

More and more evidence indicating NKT cell played a crucial role of the immune system in the development and outcome of Diffuse Large B-cell Lymphoma (DLBCL), as well as other B-cell lymphomas and solid cancers. The characteristics of the tumor microenvironment (TME) vary among different lymphoma types[15]. In DLBCL, disrupted communication between lymphoma cells and the microenvironment contributes to the ability of lymphoma cells to evade the immune system's surveillance. Immune escape mechanisms in DLBCL include: (1) altering immune recognition by reducing or losing recognition molecules, (2) suppressing the immune system's antitumor function, and (3) creating a microenvironment that supports the growth of lymphoma cells. Altering immune recognition, in particular, plays a significant role in DLBCL's tumor development and progression, prompting active investigation into its molecular foundations.

◀**Fig. 4**. Expression and immune pattern among adrenal gland samples. (**A**) Correlation plot of all adrenal gland DLBCL samples. Two clusters were observed among adrenal gland samples. (**B**) Significant different expressed genes enriched in cluster1 and cluster2. (**C**) NKT score between cluster 1 and cluster 2 adrenal gland DLBCL samples. Nonparametric Wilcoxon test was utilized for comparison, p values < 0.05 were considered significant difference. (**D**) CD4 memory T score between cluster 1 and cluster 2 adrenal gland DLBCL samples. Nonparametric Wilcoxon test was utilized for comparison, p values < 0.05 were considered significant difference. (**E**) Proliferate B cell score between cluster 1 and cluster 2 adrenal gland DLBCL samples. Nonparametric Wilcoxon test was utilized for comparison, p values < 0.05 were considered significant difference. (**F**) Differentially expressed gene enriched in KRAS pathways in multiple cancers by gene set enrichment analysis. p values < 0.05 were considered significant difference. (**G**) Differentially expressed gene enriched in ATM, P53, PTEN pathways by gene set enrichment analysis. p values < 0.05 were considered significant difference.

Conclusion

In this study, we sequenced ten DLBCL samples from adrenal gland, analyzed multiple organ related DLBCL RNA data, defined the new subtype of adrenal gland DLBCL and explore their molecular signatures. Our study expanded the organ related DLBCL data, provided the new knowledge of adrenal gland DLBCL expression profile.

Data availability

The datasets presented in this study can be available from the corresponding author on reasonable request.

Received: 5 February 2024; Accepted: 14 February 2025
Published online: 26 February 2025

References

1. Martelli, M. et al. Diffuse large B-cell lymphoma. *Crit. Rev. Oncol. Hematol.* **87**(2), 146–171 (2013).
2. Schmitz, R. et al. Genetics and pathogenesis of diffuse large B-cell lymphoma. *N. Engl. J. Med.* **378**(15), 1396–1407 (2018).
3. Vodicka, P., Klener, P. & Trneny, M. Diffuse large B-cell lymphoma (DLBCL): Early patient management and emerging treatment options. *OncoTargets Ther.* **15**, 1481–1501 (2022).
4. Dobin, A. et al. STAR: Ultrafast universal RNA-seq aligner. *Bioinformatics* **29**(1), 15–21 (2013).
5. Liao, Y., Smyth, G. K. & Shi, W. featureCounts: An efficient general purpose program for assigning sequence reads to genomic features. *Bioinformatics* **30**(7), 923–930 (2014).
6. Love, M. I., Huber, W. & Anders, S. Moderated estimation of fold change and dispersion for RNA-seq data with DESeq2. *Genome Biol.* **15**(12), 550 (2014).
7. Aran, D., Hu, Z. & Butte, A. J. xCell: Digitally portraying the tissue cellular heterogeneity landscape. *Genome Biol.* **18**(1), 220 (2017).
8. Wu, T. et al. clusterProfiler 4.0: A universal enrichment tool for interpreting omics data. *Innovation (Camb)* **2**(3), 100141 (2021).
9. Li, J. et al. NKT cell responses to B cell lymphoma. *Med. Sci. (Basel)* **2**(2), 82–97 (2014).
10. Casey, S. C. et al. Cancer prevention and therapy through the modulation of the tumor microenvironment. *Semin. Cancer Biol.* **35**(Suppl), S199–S223 (2015).
11. Wang, L. et al. Detachable nanoparticle-enhanced chemoimmunotherapy based on precise killing of tumor seeds and normalizing the growing soil strategy. *Nano Lett.* **20**(9), 6272–6280 (2020).
12. Hui, L. & Chen, Y. Tumor microenvironment: Sanctuary of the devil. *Cancer Lett.* **368**(1), 7–13 (2015).
13. Junttila, M. R. & de Sauvage, F. J. Influence of tumour micro-environment heterogeneity on therapeutic response. *Nature* **501**(7467), 346–354 (2013).
14. Bejarano, L., Jordao, M. J. C. & Joyce, J. A. Therapeutic targeting of the tumor microenvironment. *Cancer Discov.* **11**(4), 933–959 (2021).
15. Ennishi, D. The biology of the tumor microenvironment in DLBCL: Targeting the "don't eat me" signal. *J. Clin. Exp. Hematopathol.* **61**(4), 210–215 (2021).

Acknowledgements

We appreciate the support of Dr. Yunke Li from Beijing Digitf Biotechnology Co., Ltd. (Beijing) in data analysis and colleagues from Annoroad Gene Technology (Beijing, China) for technical support.

Author contributions

Weijing Jia, Ruochen Qi, Xiaoyan Zhang: Conceptualization, methodology, data analysis; Kepu Liu, Longlong Zhang: Clinical data collection; Xiaozheng Fan, Bo Yang: Writing-original draft preparation; Guohui Wang, Shichao Han, Shuaijun Ma: Supervision, writing- reviewing and editing.

Declarations

Competing interests

The authors declare no competing interests.

Ethics statement

This study was approved by the Institutional Ethics Board of The First Affiliated Hospital of Air Force Military Medical University. The studies were conducted in accordance with the local legislation and institutional requirements. Written informed consent was obtained from the patients in this study.

Additional information

Correspondence and requests for materials should be addressed to G.W., S.H. or S.M.